# Collective settling of fine particles in a narrow channel with arbitrary cross-section

Shusaku Harada[*,a], Megumi Kondo[a], Kensuke Watanabe[a], Taiga Shiotani[a], Kodai Sato[a]

[a] *Division of Sustainable Resources Engineering, Faculty of Engineering, Hokkaido University, N13W8, Sapporo, Hokkaido, 060-8628, Japan*

**Abstract**

Gravitational settling of fine particles in a liquid-filled narrow channel has been studied experimentally and theoretically. Previous studies have shown that the particulate suspension with concentration interface toward gravitational direction behaves as a continuous fluid for high concentration and small particle size, and the gravity-induced instability at the interface enhances the settling motion of particles. The purpose of this study is to investigate how such a concentration interface behaves and how particles settle by gravity in various finite-sized channels. The experimental and theoretical results indicate that the aspect ratio of the channel cross-section is an important parameter for describing the settling behavior of particulate suspension. Moreover, we predict the velocity of the collective settling of particles in channels with arbitrary cross-section.

*Key words:* Particle, Suspension, Sedimentation, Multiphase flow, Interface, Fluid mechanics

[*] Corresponding author
*Email address:* harada@eng.hokudai.ac.jp (Shusaku Harada)

## 1. Introduction

Transport of particulate materials in liquid-filled channels, such as water-saturated porous media, soils or cracks in rocks, are widely seen in industrial applications and natural phenomena. There have been numerous studies in various fields of chemical engineering (Sharma and Yortsos, 1987; Biggs et al., 2003), environmental engineering (Mondal and Sleep, 2012), mechanical and civil engineering (Adler et al., 2002). The dispersion process of materials in these channels is crucially difficult to predict quantitatively because it depends on geometric characteristics of channels in addition to fluid and particle properties. There are many parameters describing channel characteristics such as size, length, cross-sectional shape, inclination, bifurcation, confluence and so on. In most cases, these characteristics have been considered together as macroscopic properties like porosity or tortuosity (Epstein, 1989; Jury and Horton, 2004; Shen and Chen, 2007).

In particular, gravitational dispersion of particles in liquid-filled channels is commonly seen in various processes such as contaminant transport. However, even if the channel has simple geometry and the filling liquid is stationary (no advection), the gravitational motion of particulate materials is quite complicated. The particles do not always settle independently with their terminal velocity and sometimes they settle collectively (Nitche and Batchelor, 1997; Machu et al., 2001; Metzger et al., 2007). In some cases, suspended particles move with the interstitial fluid as one continuous fluid as if it is immiscible in surrounding fluid. Consequently the collectivity of suspended particles brings about the variation of the whole dispersion behaviors.

If the concentration gradient is positive in vertical direction, i.e., the upper part is denser, hydrodynamic instability (Rayleigh-Taylor instability) occurs at suspension-pure fluid interface (Völtz et al., 2000; Völtz et al., 2001; Völtz, 2003). Such instability of suspension-fluid interface greatly influences the settling motion of constituent particles. Fig.1 is the settling behavior of particulate suspension arranged in laminae for various particle and fluid conditions in quasi two-dimensional closed channel (Harada et al., 2012). If the particle size is small and the concentration is large, the suspension behaves as an immiscible fluid even though there is no definite interface and the suspended particles settle with the growth of fingering instability at lower suspension-fluid interface. In this case, the settling velocity is hundred times larger than that of an isolated particle. Therefore, the collectivity of suspended particle is quite important for quantitative prediction of gravitational dispersion of particles in channels.

The lengthscale and the growth rate of Rayleigh-Taylor instability greatly depend on the geometric condition of channels (Fernandez et al., 2001, 2002; Martin et al., 2002). In consequence, the velocity of collective settling also depends on the channel geometry. The purpose of this study is to investigate how such instability occurs in a narrow channel and how the suspended particles settle by gravity. This article indicates the importance of channel geometry, particularly cross-sectional shape, for the gravitational settling of particulate suspension in a narrow channel through the consideration of simple system.

## 2. Experimental method

Figure 2 shows the schematic diagram of experimental apparatus. The test cell is quasi-two dimensional closed channel with a height $L = 200$mm. The channel is made by acrylic plates except for the front glass. The thickness $D$ and the width $T$ of the channel are adjustable from $D$=3 to 12mm and $T$=6 to 100mm respectively. There is a horizontal slit on the back side of the channel. A thin blade is put into the slit for dividing suspension from pure fluid. The blade is made from a stainless steel plate with a thickness 0.5mm.

At first pure fluid (silicone oil) is filled into the lower part of the channel until the surface reaches the position of the slit. Then the blade is put into the channel and the suspension is filled above it. After that the blade is removed backward and the settling behavior of the suspended particles by gravity is recorded by a digital video camera.

The suspension is made of glass particles and silicone oil. The diameter of particle $d_p$ is 30$\mu$m and the mass density $\rho_p$ is 2500 kg/m$^3$. The density of the silicone oil $\rho_f$ is 972 kg/m$^3$ and the viscosity $\mu_f$ is 1.94 Pa·s. The corresponding Stokes settling velocity $U_0 = (\rho_p - \rho_f)d_p^2 g/18\mu$ is $3.85 \times 10^{-4}$ mm/s. In this experiment, the particle concentration is set to be constant and is $\phi = 0.05$. The suspension is mixed by stirring for several hours and is deaerated well in constant temperature (22$\pm$1C$^\circ$). The pure fluid which is used to fill the lower part of the channel has the same properties as constituent fluid of the suspension. Therefore the initial state can be interpreted as partially suspended particles in a static pure fluid.

After the blade is removed, the suspension-pure fluid boundary can be observed definitely (see initial conditions in Fig.3). However, there is phys-

ically no definite border because the suspension is made of the same fluid as the lower one. It should be considered that the particles are suspended partially in a static fluid. Such an ambiguous boundary between suspension and fluid is called concentration interface. At the concentration interface of micron-sized particles, the interfacial tension can be considered zero. If there is a dominant interparticle force such as van der Waals force in the system, it is possible to consider the pseudo-interfacial effect on the suspension-fluid boundary. However, it appears that there is no significant force compared to gravity force and fluid force acting on micron-sized particles we used here.

## 3. Results and discussion

### *3.1. Settling behavior of suspension*

The settling behavior of suspension was observed with keeping the channel thickness (short side) constant and changing the channel width (long side). Figure 3 shows the settling behavior of suspension for a channel thickness $D = 5$mm with various channel widths $T$. The moment the dividing blade is removed backward is set to be $t = 0$. As can be seen, finger-like instability develops at concentration interface and the settling of suspended particle is subject to macroscopic motion of the interface instabilities. As described in our previous article (Harada et al., 2012), such fingering instability is fundamentally the same as Rayleigh-Taylor instability and it behaves as immiscible fluids if the particle size is small and the concentration is high, more quantitatively phrased, if a non-dimensional parameter $d_p/\phi^{1/3}\lambda$ ($\lambda$: wave length of the instability) is less than 0.03.

It is found from Fig.3 that the settling behavior of suspension depends

on the channel width $T$. In cases of small channel width (Fig.3a, b), only one finger grows up near the center of the channel.In these cases, the width of finger is larger for larger channel width. However, if the channel width is moderate (Fig.3c), a few fingers are observed. If the channel width is adequately large (Fig.3d), many fingers grow up and the finger width does not depend on the channel width.

Figure 4 shows the change in the length of fingers with time under the same conditions as Fig.3. The fingers appear to grow in an exponential manner at the beginning and then their growth velocity becomes constant. These behaviors are similar to the Rayleigh-Taylor instability of immiscible fluids. We define the settling velocity $U_{\mathrm{exp}}$ by averaging the gradient of the change in the finger length at a later stage. We can found visually that $U_{\mathrm{exp}}$ is positively correlated with the finger width, i.e., $U_{\mathrm{exp}}$ is larger for larger finger width.

Figure 5 indicates the relation between channel width $T$ and non- dimensional settling velocity $U_{\mathrm{exp}}/U_0$ ($U_0$: Stokes settling velocity) with various channel thickness $D$. It is found that the settling velocity of suspension is hundreds of times larger than the Stokes settling velocity. The rapid settling of suspension is caused by collective effect of suspended particles. Obviously the settling velocity varies with the channel width $T$ and three regions can be identified. If $T$ is small, only one finger develops and the the settling velocity is proportional to the channel width (linear region). On the other hand, if $T$ is large, the velocity does not depend on $T$ (infinite region). In addition, there is transition region among them. In the transition region, the velocity varies widely because only a few fingers appear in the channel.

The settling velocity also varies with the channel thickness $D$. The inset pictures in Fig.5 shows the settling behavior of suspension with a large channel width ($T = 100$mm). As the channel thickness $D$ increases, the finger width enlarges and consequently the settling velocity increases. However, the velocity variation with the channel width $T$ indicate a similar tendency for constant $D$. The results showed in this section indicate that the settling behavior is greatly influenced by the geometry of channel and the settling velocity is explicitly correlated with the finger width.

*3.2. Approximate solution of finger width*

For quantitative understanding of the settling velocity of particles, it is important to predict the finger width generated in channels. Völtz et al. (2001) has reported that the instability of a suspension-fluid interface could be predicted from linear stability analysis of immiscible viscous fluids on the assumption that the upper suspension is a continuous fluid having apparent density and viscosity. Here we start the stability analysis by the method similar to them and then derive the approximate solution of most-fastest growing wave length (finger width) in a quasi-two dimensional channel, i.e., $D =$const. and $T = \infty$.

The dispersion relation for two immiscible fluids with no interfacial tension in a quasi-two dimensional channel have found in our previous article (Harada et al., 2012) and is as follows.

$$\begin{aligned} &- \left[\frac{gk}{n^2}(\alpha_1-\alpha_2)+(\beta_1+\beta_2)\right][\beta_1 q_1+\beta_2 q_2-k(\beta_1+\beta_2)] \\ &- 4k\beta_1\beta_2+\frac{4k^2}{n}(\alpha_1\bar{\nu}_1-\alpha_2\bar{\nu}_2)[\beta_1 q_1-\beta_2 q_2+k(\beta_1-\beta_2)] \\ &+ \frac{4k^3}{n^2}(\alpha_1\bar{\nu}_1-\alpha_2\bar{\nu}_2)^2(q_1-k)(q_2-k)=0, \end{aligned} \tag{1}$$

where $k$ is the wave number of disturbance and $n$ is the growth rate. $\bar{\nu}$ is kinematic viscosity and subscripts 1 and 2 indicate the lower and the upper fluid respectively. $\alpha$, $\beta$ and $q$ are defined as $\alpha_1 = \bar{\rho}_1/(\bar{\rho}_1 + \bar{\rho}_2)$, $\alpha_2 = \bar{\rho}_2/(\bar{\rho}_1 + \bar{\rho}_2)$, $\beta_1 = \alpha_1(1 + \bar{\nu}_1\eta/n)$, $\beta_2 = \alpha_2(1 + \bar{\nu}_2\eta/n)$, $q_1 = \sqrt{n/\bar{\nu}_1 + k^2 + \eta}$, $q_2 = \sqrt{n/\bar{\nu}_2 + k^2 + \eta}$ where $\eta = 12/D^2$. We set the properties of lower fluid $\bar{\rho}_1$ and $\bar{\nu}_1$ to be those of pure fluid $\rho_f$, $\nu_f$, while the properties the upper fluid $\bar{\rho}_2$, $\bar{\nu}_2$ to be apparent density and viscosity of suspension as $\rho_s = (1-\phi)\rho_f + \phi\rho_p$ and $\mu_s = (1 + 2.5\phi)\mu_f$, respectively.

Figure 6 shows the results of the growth rate $n$ for given wave number $k$ calculated by Eq.(1) under our experimental conditions. The theoretical analysis shows that the growth rate of disturbance is larger for larger channel thickness $D$. There are extreme values of growth rate on each conditions of $D$ and the wave number of maximum growth of disturbance is smaller with increasing $D$. This is consistent with the experimental fact that the width of finger is larger for larger channel thickness $D$. As mentioned below, the corresponding wave length $\lambda = k_{\max}/2\pi$ agrees quantitatively with the experimental observation of finger width (See inset pictures in Fig.7). Fig.6 indicates that the most-fastest growing wave survives among various disturbances (waves) of the initial suspension-fluid interface.

In order to examine the dependency of the instability lengthscale on the channel geometry, we derive the approximate solution of dominant wave length $\lambda$ by simplifying Eq.(1). First approximation concerns the apparent property of suspension. On the assumption of low concentration of suspension, we assume $\bar{\nu}_1 = \bar{\nu}_2$. This assumption means that the kinematic viscosity

of the suspension $\mu_s/\rho_s$ is close to that of the lower pure fluid $\mu_f/\rho_f$, i.e.,

$$\bar{\nu}_2 = \frac{(1+2.5\phi)\mu_f}{\rho_p\phi + (1-\phi)\rho_f} = \frac{1+2.5\phi}{\rho_r\phi + (1-\phi)}\bar{\nu}_1, \tag{2}$$

where $\rho_r = \rho_p/\rho_f$. On our experimental conditions ($\rho_r = 2.57$, $\phi = 0.05$), $\bar{\nu}_2 = 1.043\bar{\nu}_1$ and the assumption is almost valid. If we set $\bar{\nu}_1 = \bar{\nu}_2 = \bar{\nu}$ and $q_1 = q_2 = q$, Eq.(1) is approximately expressed as follows.

$$\begin{aligned} &- \frac{gk}{n^2}\left(\alpha_1^2 - \alpha_2^2\right)\left(1 + \frac{\bar{\nu}\eta}{n}\right)(q-k) - (\alpha_1+\alpha_2)^2\left(1+\frac{\bar{\nu}\eta}{n}\right)^2(q-k) \\ &- 4k\alpha_1\alpha_2\left(1+\frac{\bar{\nu}\eta}{n}\right)^2 + \frac{4k^2\bar{\nu}}{n}(\alpha_1-\alpha_2)^2\left(1+\frac{\bar{\nu}\eta}{n}\right)(q+k) \\ &+ \frac{4k^3\bar{\nu}^2}{n^2}(\alpha_1-\alpha_2)^2(q-k)^2 = 0 \end{aligned} \tag{3}$$

Eq.(3) is normalized by a characteristic length $L = 1/\sqrt{\eta}$ and a characteristic time $T = \bar{\nu}\sqrt{\eta}/gA$, where $A$ is Atwood number and $A = (\bar{\rho}_2 - \bar{\rho}_1)/(\bar{\rho}_2 + \bar{\rho}_1)$. The obtained equation is as follows.

$$\begin{aligned} &\left(Rn^*k^* + k^* - 4A^2Rn^{*2}k^{*2} - 4A^2n^*k^{*2}\right)\left(\sqrt{Rn^* + k^{*2} + 1} - k^*\right) \\ &- \left(R^2n^{*3} + 2Rn^{*2} + n^*\right)\left(\sqrt{Rn^* + k^{*2} + 1} - A^2k^*\right) \\ &+ 4A^2n^*k^{*3}\left(\sqrt{Rn^* + k^{*2} + 1} - k^*\right)^2 = 0 \end{aligned} \tag{4}$$

where $R = gA/\bar{\nu}^2\eta^{3/2}$ is non-dimensional parameter describing the gravity force compared to viscous force in a narrow channel. If $R \ll 1$ (small $D$) and $A^2 \ll 1$ (small density difference) are assumed, we finally obtain an approximate relation between non-dimensional wave number $k^*$ and growth rate $n^*$ as follows;

$$n^* = k^* - \frac{k^{*2}}{\sqrt{k^{*2}+1}} \tag{5}$$

By setting $dn^*/dk^* = 0$, we can calculate the wave number $k^*_{\max}$ at which the growth rate is maximum as

$$k^*_{\max} = \sqrt{\frac{\sqrt{5}-1}{2}} \tag{6}$$

Finally we obtain the analytical expression of the corresponding wave length $\lambda = 2\pi/k_{\max} = 2\pi/\sqrt{\eta}k^*_{\max}$,

$$\lambda = \frac{2\pi}{\sqrt{6\left(\sqrt{5}-1\right)}}D \tag{7}$$

It is found from Eq.(7) that the dominant wave length (finger width) $\lambda$ is approximately a linear function of the channel thickness $D$ and $\lambda = 2.31D$.

Fernandez et al. (2001, 2002) have performed the linear stability analysis of Rayleigh-Taylor instability on miscible and immiscible interfaces of pure fluids in a narrow vessel. They have found that the dominant wave lengths of miscible and immiscible interfaces are different and they depend on interfacial tension and diffusivity respectively. However, their results indicate that the wave length is asymptotically close to constant value $2.3D$ in special cases that the immiscible interface with no interfacial tension and the miscible interface with no diffusion. Eq.(7) corresponds to their special cases.

Figure 7 shows the dominant wave length of interfacial instability by numerical analysis of exact formula (Eq.(1)) and the approximate solution (Eq.(7)). Since they are in agreement very well within $D < 20$mm, the assumptions described above are reasonable for our experimental conditions. Figure 7 also shows the experimental results of finger width and the corresponding pictures. The line in each picture indicates the wave length by exact numerical solution. The finger width agrees quantitatively with theoretical

predictions and it increases with increasing the channel thickness $D$. In conjunction with the results by Fernandez et al. (2001, 2002), the concentration interface between suspension with micron-sized particles and pure fluid can be interpreted as both immiscible boundary with no interfacial tension and miscible boundary with no diffusion.

*3.3. Effect of channel geometry*

In the previous section, we showed that the dominant wave length of instability (finger width) $\lambda$ in a quasi-two dimensional channel depends on the channel thickness $D$. In this section, we consider again the finger-like settling of suspension in finite-sized channels shown in Fig.3. If the channel width (long side) $T$ is adequately larger than the thickness (short side) $D$, the instability would develop with constant wave length described in Eq.(7). On the other hand, if the channel width $T$ is comparable with the wave length $\lambda$, the instability cannot grow up with the original wave length due to the influence of the side walls. Therefore it is expected that the resulting finger width is closely related to the ratio $T/\lambda$. Meanwhile, as described in Eq.(7), the wave length $\lambda$ is proportional to the channel thickness $D$. Consequently the settling behavior of suspension in a finite-sized channel is determined by the aspect ratio of channel $T/D$.

Figure 8 shows the relation between aspect ratio of the channels and the settling velocity $U_{\exp}/U_{\infty}$. $U_{\infty}$ indicates the settling velocity in the channel with $T = 100$mm in which the effect of side walls can be neglected. The upper abscissa in Fig.8 shows $T/\lambda$. It is found that the settling velocity is well scaled by the aspect ratio $T/D$. if the aspect ratio is small ($T/D < 5$), only one finger grows up and the settling velocity increases proportional to $T$

according to the widening of the finger (linear region). For moderate aspect ratio ($5 < T/D < 15$), a few fingers develops and the velocity varies widely (transition region). When $T/D$ is large ($T/D > 15$), the finger with a fixed width (Eq.(7)) grows up and the settling velocity becomes constant (infinite region). It is concluded that the gravitational settling of suspension in a narrow channel is greatly influenced by the channel geometry and the aspect ratio is a crucial parameter for describing the settling behaviors.

Here we try to interpret the above results in terms of gravitational settling of a particle assembly (suspension blob). We consider the settling of a disk-shaped suspension blob with a diameter $L$ and a thickness $D$. The settling velocity can be calculated from the balance between the gravity and buoyancy force ($\sim \Delta\rho L^2 Dg$) and the drag force ($\sim \mu_f LU$), and consequently $U \sim \Delta\rho gLD/\mu_f$. Therefore the dependence of the settling velocity on the geometry is $U \sim LD$. If the finger can be considered as such a blob, the diameter $L$ can be replaced by the finger width, which is proportional to $T$ for small aspect ratio, and is close to $\lambda$ for large aspect ratio. Consequently, the velocity $U \sim TD$ in linear region and $U \sim \lambda D$ in infinite region. By using the linear relationship between $\lambda$ and $D$, we finally obtain the geometrical dependencies of the settling velocity, i.e., $U/U_\infty = TD/\lambda D \sim TD/D^2 = T/D$ for linear region, and $U/U_\infty = \lambda D/\lambda D$ =const. in infinite region. These results coincide with the measured results shown in Fig.8. Therefore the collective settling of particles in narrow channels can be interpreted roughly as the settling of an apparent blob.

*3.4. Prediction of settling velocity in arbitrary channel*

We propose the prediction method of the settling velocity of fine particles in arbitrary channels. Before that, we reconsider the experimental results of the gravitational settling of various-sized particles described in our previous article (Harada et al., 2012). Fig.9 is the settling velocity of particles in quasi-two dimensional closed channels. They are obtained from 14 kinds of experiment for various particle and fluid properties. The short side length of the channel $D$ is variable from 3 to 8mm and the long side length $T$ is constant and set to be 100mm, which is adequately long compared to the short side. Therefore the geometrical condition of the channel corresponds to "infinite region" in Fig.8. We reported in the article that if non-dimensional parameter $d_p/\phi^{1/3}\lambda$ is less than 0.03, the suspended particles settle as one continuous fluid (fluid-like settling).

It is found from Fig.9 that the velocity of the collective settling normalized by Stokes settling velocity $U_0$ is almost scaled by $(d_p/\phi^{1/3}\lambda)^{-2}$. This scaling can be explained as follows. From similar discussion to the previous section, the settling velocity of a finger-like blob can be roughly expressed as $U_\infty \sim \Delta\rho g\lambda D/\mu_f \sim \phi(\rho_p - \rho_f)g\lambda^2/\mu_f$. On the other hand, Stokes settling velocity can be expressed as $U_0 \sim (\rho_p - \rho_f)gd_p^2/\mu_f$. Consequently the velocity ratio can be expressed as $U_\infty/U_0 \sim \phi\lambda^2/d_p^2$. This is almost the same as $(d_p/\phi^{1/3}\lambda)^{-2} = \phi^{2/3}\lambda^2/d_p^2$ except for insensitive function $\phi^{1/3}$. As can be seen in Fig.9, the settling velocity in fluid-like region can be fitted well by $U_\infty/U_0 = 0.02(d_p/\phi^{1/3}\lambda)^{-2}$.

Here we give a prediction procedure for the velocity of fine particles which settle collectively in a vertical channel with arbitrary cross-section. From

Eq.(7), the finger width can be determined by the short side length of the channel, i.e., $\lambda = 2.31D$. Therefore the unspecified variable $\lambda$ can be immediately replaced by specified value $D$ in the above discussions. That is, if the non-dimensional parameter $d_p/\phi^{1/3}D$ is less than the threshold of collective (fluid-like) settling $d_p/\phi^{1/3}D = 0.069$, the suspended particles settle as a continuous fluid in a quasi-two dimensional channel and the settling velocity is expressed as follows.

$$U_\infty = 0.107(d_p/\phi^{1/3}D)^{-2}U_0 \tag{8}$$

Once $U_\infty$ is obtained, we can predict the settling velocity in the channel with arbitrary cross-section from Fig.8.

As an example, we demonstrate the calculation of the settling velocity of glass particles ($\rho_p$ = 2500kg/m$^3$, $d_p$=30$\mu$m, $\phi$=0.05) in a vertical channel with cross-section ($D$,$T$)=(5,12) (unit:mm). Under these conditions, the particles behave perfectly collective (fluid-like) because $d_p/\phi^{1/3}D = 0.016$ which is smaller than 0.069. The settling velocity for ($D$,$T$)=(5,$\infty$) can be calculated as $U_\infty = 0.107(0.016)^{-2}U_0 = 418U_0$. On the other hand, the geometrical condition for $T/D = 12/5 = 2.4$ corresponds to linear region and the settling velocity is approximately $U = 0.75U_\infty$ from Fig.8. Finally we can calculate the velocity as $U = 314U_0 = 0.121$mm/s, which is close to the measured value 0.136mm/s.

## 4. Conclusions

The gravitational settling of particulate suspension in a narrow channel has been investigated. On our experimental conditions, the settling behavior of suspended particle is completely fluid-like and the settling velocity

is dominated by downstream flow caused by the gravity-induced instability. The results indicate that the aspect ratio of the channel cross-section is an important parameter for describing the settling behavior of particulate suspension in a narrow channel. Our results suggest that, if we predict the gravitational dispersion of particulate materials in liquid-filled channels, the cross-sectional shape of channel should be considered as one of crucial parameters for dispersion process.

## 5. Acknowledgment

This work has been partly supported by the Grant-in-Aid for Scientific Research (C) 23560178, Japan Society for the Promotion of Science.

## References

Adler, P. M., Thovert, J.-F., Bekri, S. and Yousefian, F., *J. Eng. Mech.* (2002), **128**, 829–839.

Biggs, M. J., Humby, S. J., Buts, A. and Tüzün, U., *Chem. Eng. Sci.* (2003), **58**, 1271–1288.

Epstein, N., *Chem. Eng. Sci.* (1989), **44**, 777–779.

Fernandez, J., Kurowski, P., Limat, L. and Petitjeans, P., *Phys. Fluids* (2001), **13**, 3120–3125.

Fernandez, J., Kurowski, P., Petitjeans, P. and Meiburg, E., *J. Fluid Mech.* (2002), **451**, 239–260.

Harada, S., Mitsui, T. and Sato, K., *Eur. Phys. J. E* (2012), **35**, 1–6.

Jury, W. A. and Horton, H., *Soil Physics*, John Wiley, (2004).

Machu, G., Meile, W., Nitche, L. C. and Schaflinger, U., *J. Fluid Mech.* (2001), **447**, 299–336.

Martin, J., Rakotomalala, N. and Salin, D., *Phys. Fluids* (2002), **14**, 902–905.

Metzger, B., Nicolas, M. and Guazzelli, E., *J. Fluid Mech.* (2007), **580**, 283–30.

Mondal, P. K. and Sleep, B. E., *Env. Sci. Tech.* (2012), DOI:10.1021/es301721f.

Nitche, J. M. and Batchelor, G. K., *J. Fluid Mech.* (1997), **340**, 161–175.

Sharma, M. M. and Yortsos, Y. C., *AIChE J.* (1987), **33**, 1636–1643.

Shen, L. and Chen, Z., *Chem. Eng. Sci.* (2007), **62**, 3748–3755.

Völtz, C., Schröter, M., Iori, G., Betat, A., Lange, A., Engel, A. and Rehberg, I., *Phys. Rep.* (2000), **337**, 117–138.

Völtz, C., Pesch, W. and Rehberg, I., *Phys. Rev. E* (2001), **65**, 011404.

Völtz, C., *Phys. Rev. E* (2003), **68**, 021408.

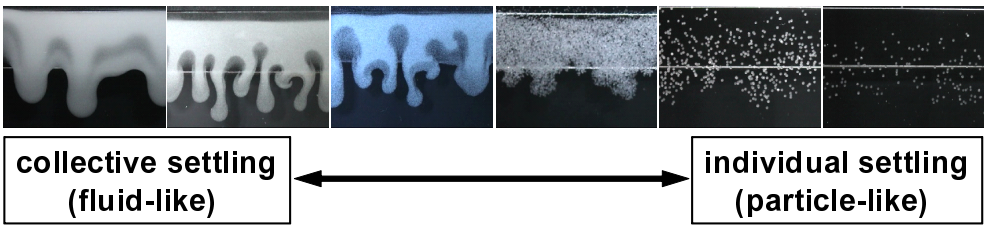


Figure 1: Settling behavior of stratified suspension in quasi two-dimensional vessel for various particle and fluid properties. Detailed conditions are described in Harada et al. (2012).

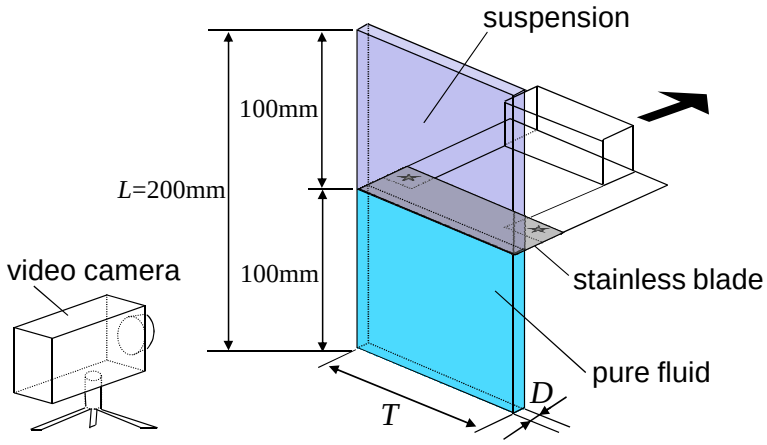


Figure 2: Schematic diagram of experimental system. Short side length $D$ varies from 3 to 12mm, while long side length $T$ varies from 6 to 100mm.

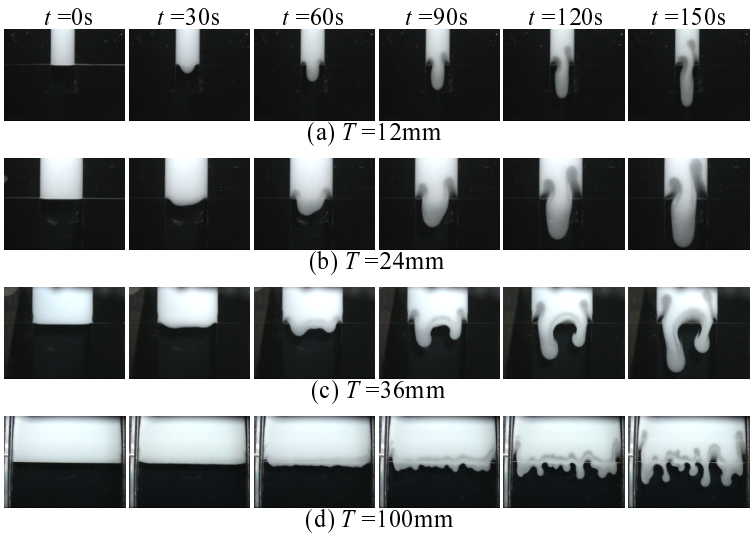


Figure 3: Settling behavior of particulate suspension with various channel width $T$ for channel thickness $D = 5$mm.

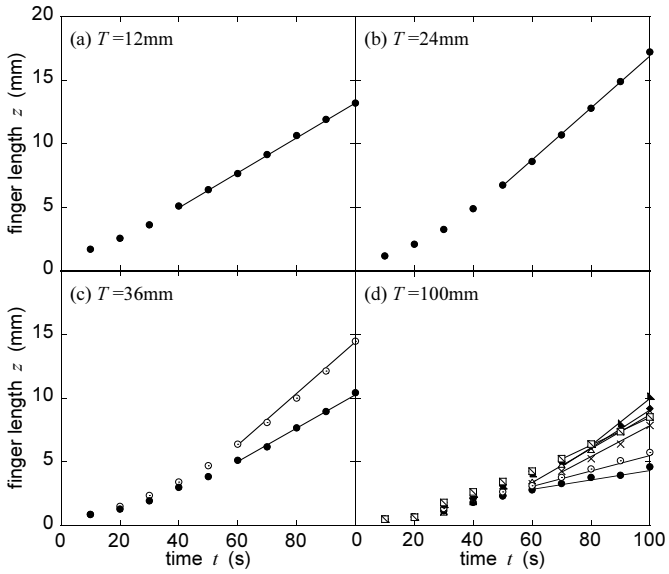


Figure 4: Change in finger length with time. (a)-(d) correspond to those in Fig.3.

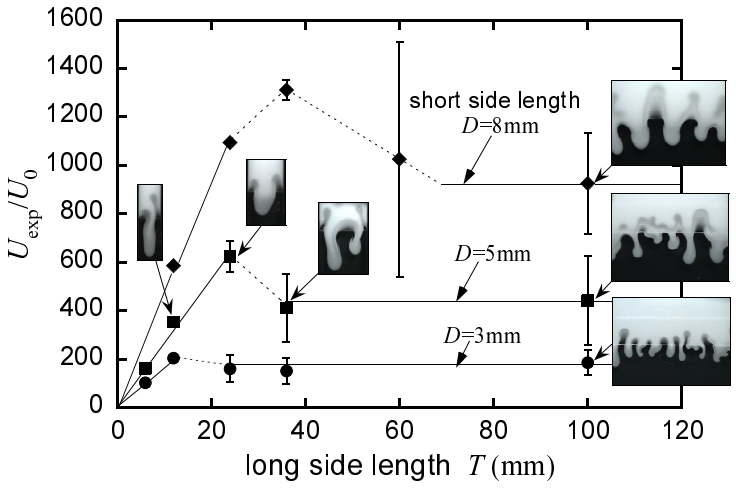


Figure 5: Relation between channel width $T$ and non-dimensional settling velocity $U_{\exp}/U_0$

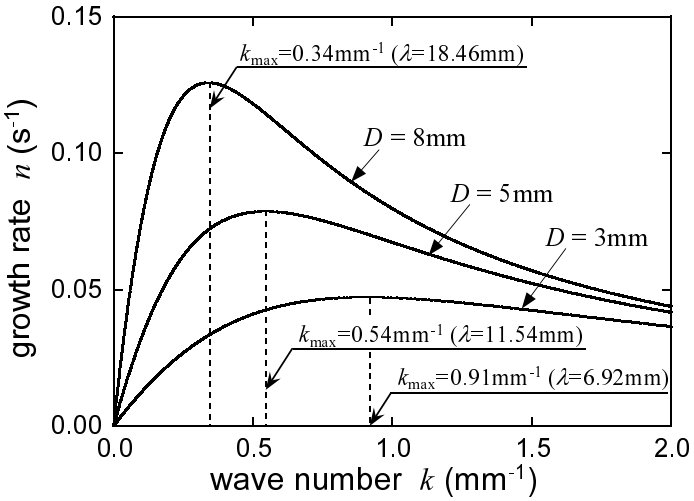


Figure 6: Relation between wave number and growth rate by linear stability analysis. Dotted line indicates the wave number of maximum growth and $\lambda(= 2\pi/k_{\max})$ is the corresponding wave length.

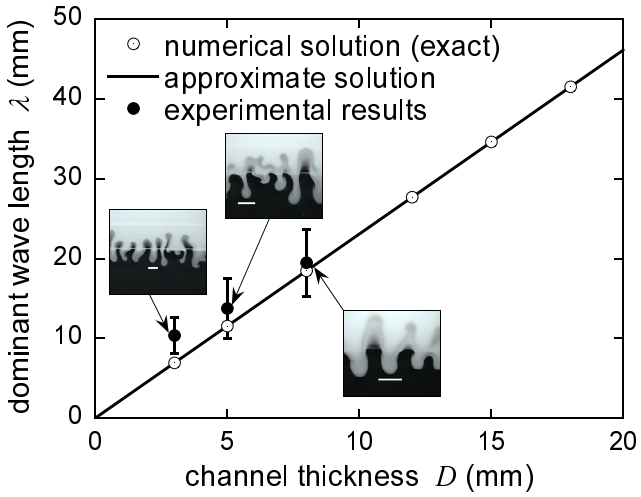


Figure 7: Dominant wave length of interfacial instability; numerical solution of exact formula (Eq.(1)), approximate solution (Eq.(7)) and experimental results of finger width. The line in each picture indicates the wave length by exact numerical solution.

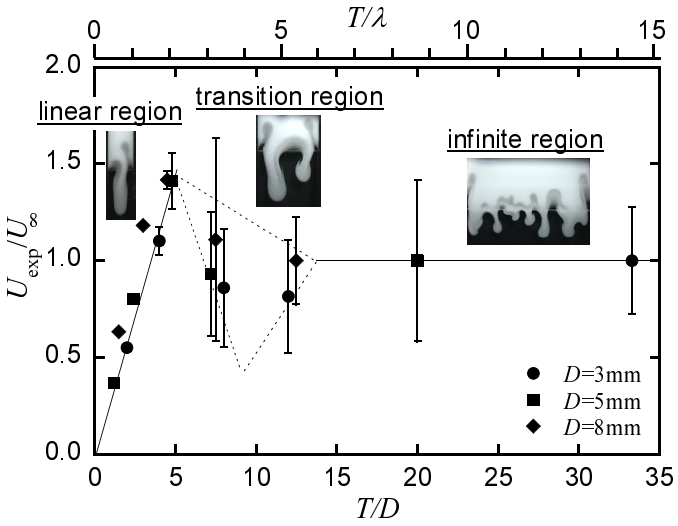


Figure 8: Relation between aspect ratio $T/D$ and non-dimensional settling velocity $U_{\mathrm{exp}}/U_{\infty}$. The upper axis indicates normalized channel width by dominant wave length $T/\lambda$.

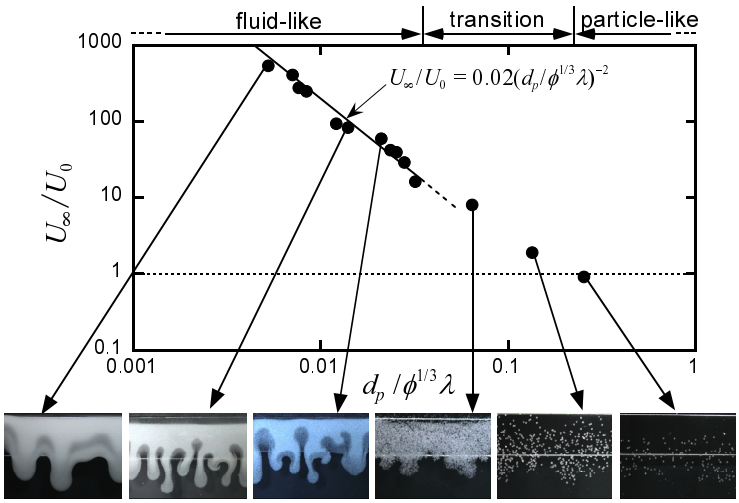


Figure 9: Relation between non-dimensional parameter $d_p/\phi^{1/3}\lambda$ and non-dimensional velocity $U_\infty/U_0$ for channel long side $T = 100$mm (constant) and short side $D = 3$ to 8mm (Reconstruction of Fig.6 in Harada et al. (2012)).